Carbohydrate Polymers 117 (2015) 414–421

Contents lists available at ScienceDirect

Carbohydrate Polymers

journal homepage: www.elsevier.com/locate/carbpol

Fabrication of cellulose self-assemblies and high-strength ordered cellulose films

Zaiwu Yuan[a,*], Jingjing Zhang[a], Anning Jiang[a], Wenting Lv[a], Yuewen Wang[a], Hongjuan Geng[a], Jin Wang[a], Menghua Qin[b,*]

[a] Key Laboratory of Fine Chemicals in Universities of Shandong, Qilu University of Technology, Jinan 250353, China
[b] Laboratory of Organic Chemistry, Taishan University, Taian 271021, China

ARTICLE INFO

Article history:
Received 28 August 2014
Received in revised form 2 October 2014
Accepted 5 October 2014
Available online 12 October 2014

Keywords:
Cellulose
Self-assembly
Cellulose film
Ordered-structure
High-strength

ABSTRACT

Based on the formation of cellulose hydrogels in NaOH/urea aqueous solvent media, cellulose self-assembly precursor is acquired. It is proved that the water uptake capability of the cellulose hydrogels depends highly on the cross-link degree (CLD) of cellulose. With varying CLD and concentration of cellulose, a variety of morphologies of cellulose self-assemblies, including sheets with perfect morphology, high-aspect-ratio fibers, and disorganized segments and network, are formed through evaporation. Furthermore, cellulose films are fabricated by diecasting and evaporating the cellulose hydrogels, resulting in a 3D-ordered structure of closely stacking of cellulose sheets. The mechanical test indicates both tensile strength and flexibility of the cellulose films are greatly improved, which is attributed to the formation of the orderly stacking of cellulose sheets. The study is expected to lay an important foundation on the preparation of ordered and high-strength cellulose materials.

1. Introduction

As the main constituent of wood and plants, cellulose is an almost inexhaustible polymeric raw material on the earth. It has a fascinating structure and is highly biocompatible and easily biodegradable. It was reported that the elastic modulus of the crystalline region of cellulose might reach the level as high as 100–200 GPa, and the density as low as 1.6 g cm^{-3} (Šturcová, Davies, & Eichhorn, 2005; Moon, Martini, Nairn, Simonsen, & Youngblood, 2011; Eichhorn, 2012). These excellent properties make cellulose a focus of current researches in material preparation (Chang, Duan, & Zhang, 2009; Morandi, Heath, & Thielemans, 2009; Saito, Uematsu, Kimura, Enomae, & Isogai, 2011; Chen, Yu, Li, Liu, & Li, 2011; Fox et al., 2012). Especially, due to possessing large amounts of hydroxyl groups, cellulose is a good object for chemical modification, which endows it a wider range of applications, such as being used as reinforcement, thickener, emulsifier, and stabilizer, etc (Habibi, Chanzy, & Vignon, 2006; Sun, Sun, Wei, Liu, & Zhang, 2007; Shahin, Nicolai, Benyahia, Tassin, & Chassenieux, 2013). Up to date, cellulose is becoming one of the most promising candidates to replace petroleum-based materials in both daily life and industry production.

However, comparatively strong H-bonds between cellulose chains would be formed because of the abundant hydroxyl groups on cellulose. Therefore, a quite firm network can be established in cellulose, leading to poor solubility of cellulose in both aqueous media and most of common organic solvents. This inhibits its further application. Moreover, although cellulose has been investigated to a large extent, due to the complexity of H-bonds, its fine structural features have not been identified with absolute clarity (Kroon-Batenburg & Kroon, 1997; Langan, Nishiyama, & Chanzy, 1999; Nishiyama, Langan, & Chanzy, 2002).

Therefore, one of attractive issues on cellulose is to search for its solvent systems. As for that, a few solvents have been developed, such as *N*,*N*-dimethylacetamide (DMAc)/LiCl system, *N*-methylmorpholine *N*-oxide (NMMO)/water system, and ionic liquids, etc (Roder, Morgenstern, Schelosky, & Glatter, 2001; Swatloski, Spear, Holbrey, & Rogers, 2002; Kulpinski, 2005; Zhu et al., 2006). The dissolution of cellulose in these systems is attributed to the coordination effect between hydroxyl groups and some certain small ions (e.g., chloride ions, sodium ions, and so

* Corresponding authors at: Key Laboratory of Fine Chemicals in Universities of Shandong, Qilu University of Technology, Daxue Road, Western University Science Park, Jinan 250353, China. Tel.: +86 531 89631208/+86 538 8711009; fax: +86 531 89631111/+86 538 6715521.
E-mail addresses: yuanzaiwu@163.com (Z. Yuan), qmh@qlu.edu.cn (M. Qin).

http://dx.doi.org/10.1016/j.carbpol.2014.10.003
0144-8617/

on). As one of 'green' solvents, the NaOH/urea/water system has been paid much attention to recently because of the comparatively simple and rapid dissolving process (Cai & Zhang, 2006; Cai et al., 2008). In the solvent, urea, which plays a role of inclusion around cellulose molecules, inhibits the aggregation of cellulose Cai & Zhang, 2005). This is known as a pioneering work on further utilization of cellulose (Liu et al., 2008; Li et al., 2010; Shi et al., 2011; Cai et al., 2012; He, Xu, & Zhang, 2013; He et al., 2014). However, in all of these solvent systems, serious problems may still exist in the preparation of cellulose materials due to the strong H-bond interaction. Generally, random flocculi without any strength could be formed when a cellulose solution is diluted by water, due to the sharp change of the micro-environment around cellulose molecules. Besides, unordered hydrogels would come into being when a cellulose solution is dipped into a certain coagulating bath, resulting in final unordered dried cellulose materials (Zhang, Mao, Zhou, & Cai, 2005; Geng et al., 2014).

However, in fact, cellulose has the potential to construct ordered structure via self-assembly. For example, naturally occuring cellulose possesses a semi-crystalline structure where highly ordered regions (crystallites) distribute within unordered domains (amorphous phase). Both crystalline and amorphous regions together construct an ordered rodlike (or fibrous) structure with high aspect ratio. This is the common morphology of cellulose in nature (such as in plant cell, bacteria and some sea animals (tunicates)), which plays an important role in protecting and supporting living cells. Another typical example is the self-assembly of cellulose nanocrystals (CNCs). When reaching a certain concentration in aqueous media, CNCs are able to self-assemble into cholesteric liquid crystalline phase (Shopsowitz, Qi, Hamad, & MacLachlan, 2010; Shopsowitz, Hamad, & MacLachlan, 2012; Giese et al., 2013). In the latest researches, it has also been shown that a 2D sheet-like skeleton structure can be produced by carefully controlling the content of CNCs (Heath & Thielemans, 2010; Chen et al., 2011; Han, Zhou, Wu, Liu, & Wu, 2013). Yet for regenerated cellulose originating from dissolved cellulose, an unordered 3D network rather than ordered or organized cellulose structures would form because of the fast physical aggregation of cellulose molecules during regenerating process due to the strong H-bond interaction.

In our opinion, a possible approach to obtain or control ordered structures of regenerated cellulose is to restrain the rapid physical aggregation caused by strong H-bond interaction within dissolved cellulose. In this work, NaOH/urea aqueous media is selected as the solvent of cellulose because of its unique merits. In order to inhibit cellulose from quick flocculation when changing pH, or from unordered gelation in coagulation baths, cellulose molecules would be chemically cross-linked in the solvent media before the subsequent self-assembling. Then a 'top-down' method (ultrasonication) is adopted to shred the cellulose hydrogels, resulting in cellulose assembling precursor. The anchored cellulose matrix in the hydrogels restricts the strong H-bond interaction and causes the effect of steric hindrance which would prevent the rapid aggregation of cellulose in subsequent evaporation process. Therefore, ordered cellulose self-assemblies might be spontaneously formed during the slow dehydration of cellulose.

Relying on the above strategy in this study, two ordered structures, namely, high-aspect-ratio fibers and cellulose sheets, as well as the transitional states between them, have been observed. Furthermore, the ordered cellulose structures are employed to prepare 3D films of highly ordered structure and high strength. The study is expected to lay a foundation on fabricating ordered and high-strength cellulose materials. The study devotes to the investigation on the rules of cellulose self-assembling and the control mechanism of cellulose ordered structures. Meanwhile, we believe that the work would help to understand the deposition behavior and hierarchical alignment of cellulose in organisms.

2. Experimental

2.1. Chemicals and reagents

The high-purity cellulose, cotton linter pulp, is a gift from Yinying Chemical Firer Co. Ltd. (Gaomi, Shandong Province, China). The cellulose is of average polymerization degree of ~525. NaOH and urea of analytical reagent grades are obtained from Shanghai Chemical Reagent Co. Ltd. *N*,*N*′-methylene bisacrylamide (MBA) is a product of Fuchen Chemical Reagents Factory (Tianjin China). All of them are used directly, without further purification.

2.2. Preparation of cellulose hydrogels in aqueous solvent media

At first, a 7 wt% NaOH/12 wt% urea aqueous solution is pre-cooled to −12 °C, and then the weighted cotton linter pulp is added and stirred under the temperature of 0–4 °C. After adequate dissolution of the cotton linter pulp for 5 min, the aqueous dispersion is centrifuged at 4000 rpm for 10 min to eliminate the small quantities of residual undissolved cellulose crystals and the suspending bubbles. Thereafter, a transparent aqueous solution of ~3% cellulose is obtained.

MBA powders of various known weights are directly added into different vessels of the above cellulose aqueous solutions at room temperature. An agitation of 30 min is needed to ensure homogeneous mixing between cellulose and MBA powder. The dispersions are left at room temperature for 4 h, during which the cloudy dispersions become transparent gradually. Finally, solid-like cross-link blocks (cellulose hydrogels) are formed, indicating that cellulose has been grafted with MBA.

In order to eliminate NaOH and urea encapsulated in cellulose hydrogels, the hydrogels are soaked in a large amount of deionized water for two days, which would be replaced by fresh deionized water frequently, until pH reaches ~7. In that way, cellulose hydrogels rich in water are prepared.

2.3. Acquirement of cellulose self-assembly precursors

Cellulose self-assembly precursors are acquired by a top-down method. To be specific, 10 g cellulose hydrogels are shredded by ultrasonicating in 0 or 100 mL of deionized water using Scinenz-IID ultrasound shredder (Scinenz Biotechnology Co., LTD, Ningbo, China) with a 6 mm probe at 60% amplitude for 2 min. In this way, each of cellulose hydrogels is smashed into a mass of small cellulose elements stably suspending in water, which is used as a self-assembly precursor subsequently.

2.4. Preparation of cellulose self-assemblies

Cellulose suspensions are freeze-dried to clearly determine the morphologies of cellulose self-assemblies. Here, cellulose suspensions are pre-cooled in advance in a refrigerator, and then transferred to a cold well of −50 °C equipped with a vacuum-pumping device. After 12 h of freeze–drying, cellulose self-assemblies are formed.

2.5. Preparation of 3D cellulose films of highly ordered structure

3D cellulose films are prepared using a templating method. After homogeneous mixing between the aqueous solutions of 3% cellulose and MBA powders with $r = 0.375$, 0.473, and 0.545, the dispersions are cast into cuboid glass grooves. Thus, rectangular cellulose hydrogel films are first obtained after 4 h of chemical cross-linkage. Afterwards, the hydrogel films are soaked in deionized water for 2 days to eliminate NaOH and urea. Finally, the hydrogel films are sandwiched between two parallel glasses

(putting a 500 g weight on the glasses) and dried for 24 h under a constant temperature of 30° C and a constant humidity of 65%.

2.6. Characterizations and tests

Cellulose morphologies are examined by scanning electron microscopy (SEM, JEOL JMS-6700). Dried cellulose powders or fractured films are coated with gold by low-vacuum sputter coating technique. Fourier-transform infrared spectroscopy (FTIR) measurements are carried out on a Nexus 670 infrared spectrometer (Thermo-nicolet electron corporation, USA) using a KBr-disk method. X-ray diffraction (XRD) measurements are carried out by an X-ray diffractometer using a Cu-K_α target at 40 kV and 30 mA. The mechanical strength of cellulose films, with a dimension of 0.4 cm × 5 cm and a thickness of 38–40 μm, is measured using a universal testing machine (Jinan Tianchen Testing Machine Manufacturing Co., Ltd, China) at a crosshead speed of 1 mm min^{-1} and a gauge length of 2 cm. At least five specimens are measured for each type of films to ensure the accuracy and reproducibility.

3. Results and discussion

3.1. Self-assemblies of cellulose assisted by the cross-linkage of MBA

To prepare high-strength and high modulus cellulose materials, it is necessary to acquire ordered structures of cellulose in advance. Because of various methods of dissolving cellulose developed in recent years, to obtain dissolved cellulose molecules from natural cellulose is becoming comparatively easier. Therefore, our main strategy is to fabricate 3D ordered cellulose materials using 'dissolved' cellulose molecules with the 'bottom up' method. From those current approaches to dissolving cellulose, an easy and green one using pre-cooled NaOH/urea/water system is chosen. However, to implement the strategy, a key challenge has to be faced. To be specific, when dissolved cellulose is regenerated from aqueous solutions, the rapid flocculation of cellulose would occur if pH is sharply changed. Even if a certain coagulation bath has been adopted, in any case, 'unordered' hydrogels can only be formed, resulting in final unordered dry cellulose materials in the subsequent dehydration process.

Essentially, cellulose has the potential to self-assemble in order as mentioned above. In our view, the key factor for successful self-assembling orderly of cellulose depends on whether the strong H-bond within cellulose can be restrained, such as the cases restrained by electrostatic repulsion or by steric hindrance effect. In addition, in organisms, the formation of a relatively organized structure of cellulose fibers depends on a quite slow biosynthesis process. In the case of regenerated cellulose from dissolved cellulose, however, strong H-bond interaction within cellulose occurs too rapidly to make them orient in a more organized manner. In other words, the ordered self-assembly is impeded by numerous and comparatively intense H-bonds between cellulose molecules.

To restrain the H-bond interaction between dissolved cellulose, in this work, MBA is used to cross-link cellulose molecules. As a result of the cross-linkage effect on cellulose molecules, the positions of cellulose molecules keep relatively fixed with each other, giving rise to a steric hindrance effect within cellulose, so the great influence of H-bonds on unordered flocculation is under control.

At first, we test the reaction activity of MBA alone in NaOH/urea system contrastively. It could be observed that no change is seen for MBA powder dispersions within one month, indicating the chemical reaction does not occur for MBA in the absence of cellulose in NaOH/urea system. However, for NaOH/urea systems containing both cellulose and MBA powder, MBA powder would vanish relatively faster within 4 h. One would see that the cloudy dispersions become transparent and at the same time lose their initial fluidity gradually. The liquid dispersions would change into solid hydrogels in the end. This shows the high activity of cross-link reaction between MBA and cellulose in NaOH/urea systems. It is also noted that the cross-link reaction between MBA and cellulose occurs easily in NaOH/urea aqueous media, even without adding any initiators. Therefore, here the NaOH/urea media is apparently both a solvent of cellulose as well as a catalyst on the cross-link reaction between cellulose and MBA. Fig. 1 gives a schematic diagram that shows that dissolved cellulose is first cross-linked by MBA, and then the formed hydrogels are washed and then shredded into small elements for the subsequent self-assembling via dehydration. From Fig. 1, it is also observed that, with crossed polarizers, the hydrogels present comparatively stronger birefringent phenomenon than the initial aqueous solutions of cellulose (not shown in Fig. 1). The birefringent phenomenon should mainly result from the recrystallization of the chemical cross-linked cellulose instead of the original cellulose crystals, since the vast majority of undissolved cellulose crystals have been eliminated via centrifugal separation. Due to the H-bond interaction restrained by the steric hindrance effect of cellulose molecules, the dispersions prepared from shredded cellulose hydrogels are transparent and could keep long term stability without further flocculation.

Table 1
Weight ratios (r) of MBA to total weight of cellulose and MBA in three typical cellulose hydrogels with different CLD, and the morphological transition of cellulose self-assemblies for concentrated and diluted dispersions, respectively.

Hydrogel samples	H1	H2	H3
Weight ratios (r)	0.375	0.473	0.545
Concentrated dispersions	Sheets	Sheets	Sheets
Diluted dispersions	Network	Network + fibers	Fibers

Despite of no accurate data, the cross-link degree (CLD) of cellulose can be conveniently controlled by the addition amount of MBA. Three typical cellulose hydrogel samples marked with H1, H2, and H3, which represent growing CLD, are prepared. The corresponding weight ratios of MBA to total weight of cellulose and MBA ($r = w_{MBA}/(w_{cellulose} + w_{MBA})$) in the hydrogels (H1, H2, and H3) are 0.375, 0.473, and 0.545, respectively (Table 1). Both concentrated and diluted dispersions, which are prepared from powerful sonification of the three hydrogels in 0 and 10 times volume of water, respectively, are slowly evaporated by freeze–drying, resulting in the aggregation or self-assembly of cellulose. Fig. 2 shows the SEM images of a series of samples, from which the morphological transmutation of cellulose self-assemblies is observed. When no MBA is added, cellulose aggregates are characterized as morphological disorganization (Fig. 2a), while the addition of a small quantity of MBA induces the cellulose to orient in a slightly higher order (Fig. 2b). Thus, it is obvious that the cross-linkage for cellulose is tightly related to its organization in higher order during the dehydration process. With increasing MBA amount, the morphology of cellulose self-assemblies would transit from an interwoven fibrous network to a sheet-like skeleton. Obviously, the arrangement order is further enhanced by increasing the CLD of cellulose molecules. Such a detail is also noticed that, the three cellulose samples with different CLD are nearly identical in morphology except that the cross sections are markedly different. A comparatively rough cross section is exhibited when less MBA is used (Fig. 2f), which is expected to possess a lot of mesopores within the cellulose sheets. Meanwhile, for cellulose cross-linked using more MBA, a dense and smooth cross section appears. It is possible that the shift in morphology of cellulose sheets is due to the change in the degree of crystallinity (DC) of cellulose. Fig. S1 indicates the X-ray diffraction patterns of cellulose cross-linked by MBA, from which not only the diffraction

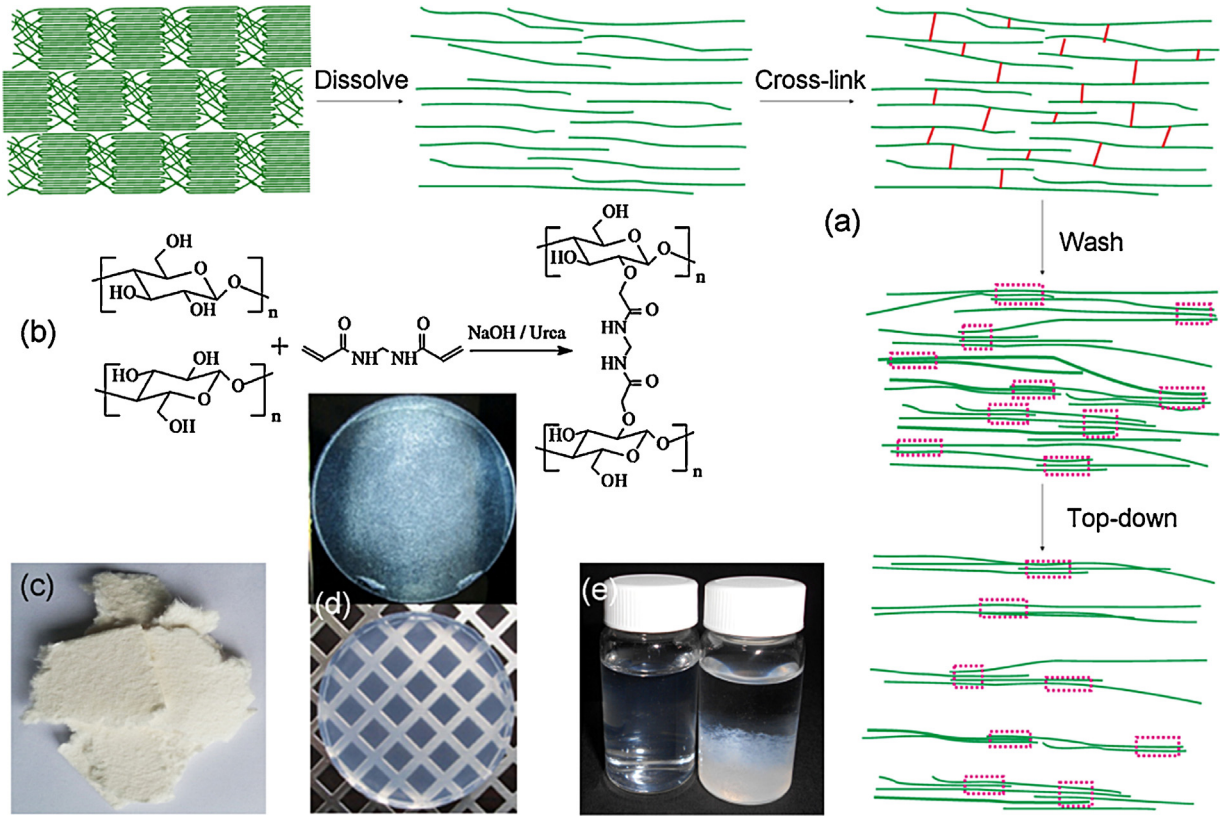

Fig. 1. (a) Schematic diagram of preparing cellulose self-assembly precursor via dissolving, cross-linking, washing, and top-down processes, respectively. The red dot boxes represent the microcrystalline areas formed in cellulose hydrogels; (b) chemical equation of the cross-link reaction between cellulose and MBA in NaOH/urea aqueous media; (c) a photograph of cotton linter pulp; (d) a photograph of cellulose hydrogels prepared via cross-linking and washing processes. The top side is the hydrogel observed with crossed polarizers; (e) the left side image is an aqueous dispersion of the shredded cellulose hydrogels, and the right is the flocculi formed by dissolved cellulose when diluted by pure water. (For interpretation of the references to color in this figure legend, the reader is referred to the web version of this article.)

peaks largely shift compared with natural cellulose, but also the peak intensity decreases with the increasing amount of MBA. This could be attributed to two reasons: on the one hand, quantities of hydroxyl groups are substituted by MBA, leading to the breakdown of the lattice structure of cellulose; on the other hand, the strong cross-linking effect limits the formation of crystalline lattice in cellulose. It could be inferred that although cellulose has been significantly cross-linked, it still displays the ability of self-assembly through slowly drying. Thus the comparatively perfect sheets could be formed. In the control experiment, however, only disorder and unshaped structure can be seen for cellulose cross-linked by no or a smaller amount of MBA.

In addition to the influence of CLD, the effect of cellulose concentrations on the self-assemblies is also investigated. SEM images in Fig. 3 show that at a low concentration of cellulose dispersions, cellulose with higher CLD tends to self-assemble into fibers with considerably high aspect ratio; for the samples with lower CLD, however, only disordered and broken cellulose sheets are obtained. Although the mechanism is not well understood up to now, it can be seen that the morphologies of cellulose self-assemblies are closely related to the cross-linked degree of cellulose.

IR spectrum in Fig. S2 shows that, for pure MBA, the strong stretching absorption of C=C bonds can be observed at 1627–1658 cm^{-1}. For cellulose grafted with MBA, however, the absorption peaks of C=C bonds disappear, even for those with higher MBA content. This indicates that C=C bonds of MBA have involved in the cross-link reaction with cellulose. On the other hand, the bending vibration absorption of N—H bonds at 1545 cm^{-1} is enhanced gradually with increasing MBA content, also indicating that MBA molecules are grafted onto cellulose. With regard to the characteristic absorption peaks of cellulose cross-linked by a certain amount of MBA, little changes have occurred at 897 cm^{-1} (due to the C—O—C stretching vibrations of $\beta(1\rightarrow4)$-glycosidic linkages), indicating cellulose chains are not broken. However, the peak at 1430 cm^{-1}, which is attributed to the stretching vibrational absorption of CH_2–OH, is obviously influenced by the grafting of MBA. In other words, the peak becomes extremely weak so that it could hardly be observed possibly because the active primary hydroxyl groups at the C-6 position preferentially take part in addition reaction with MBA. Therefore, the grafting reaction between MBA and cellulose induces two effects: (1) the H-bonding interaction within cellulose would inevitably weaken because of the loss of primary hydroxyl groups at C-6 positions, leading to the decrease of crystalinity degree of cellulose; (2) concomitantly, due to the weakened H-bond interaction between cellulose molecules, a structural transition of cellulose would occur from an initial disorder network to a perfect 2D sheet-like structure.

In addition to the shift in the morphologies of cellulose self-assemblies, water uptake capability changes greatly depending on the CLD of cellulose. When the weight ratio of MBA (r) is below 0.375, because of strong H-bond interaction within cellulose, drastic aggregation and crystalization of cellulose occur and the water uptake capability decreases. From Fig. S3, water uptake capability of the hydrogel samples is relatively low with r below 0.375, since the weight of hydrogels almost unchanges after a full soak in water, during which NaOH and urea are eliminated and pure water is trapped into cellulose matrix. With increasing content of MBA, cellulose begins to show sharp rise in its water uptake capability when r varies from 0.375 to 0.473. It is believed that the amorphous regions, which dominate the water uptake capability generally,

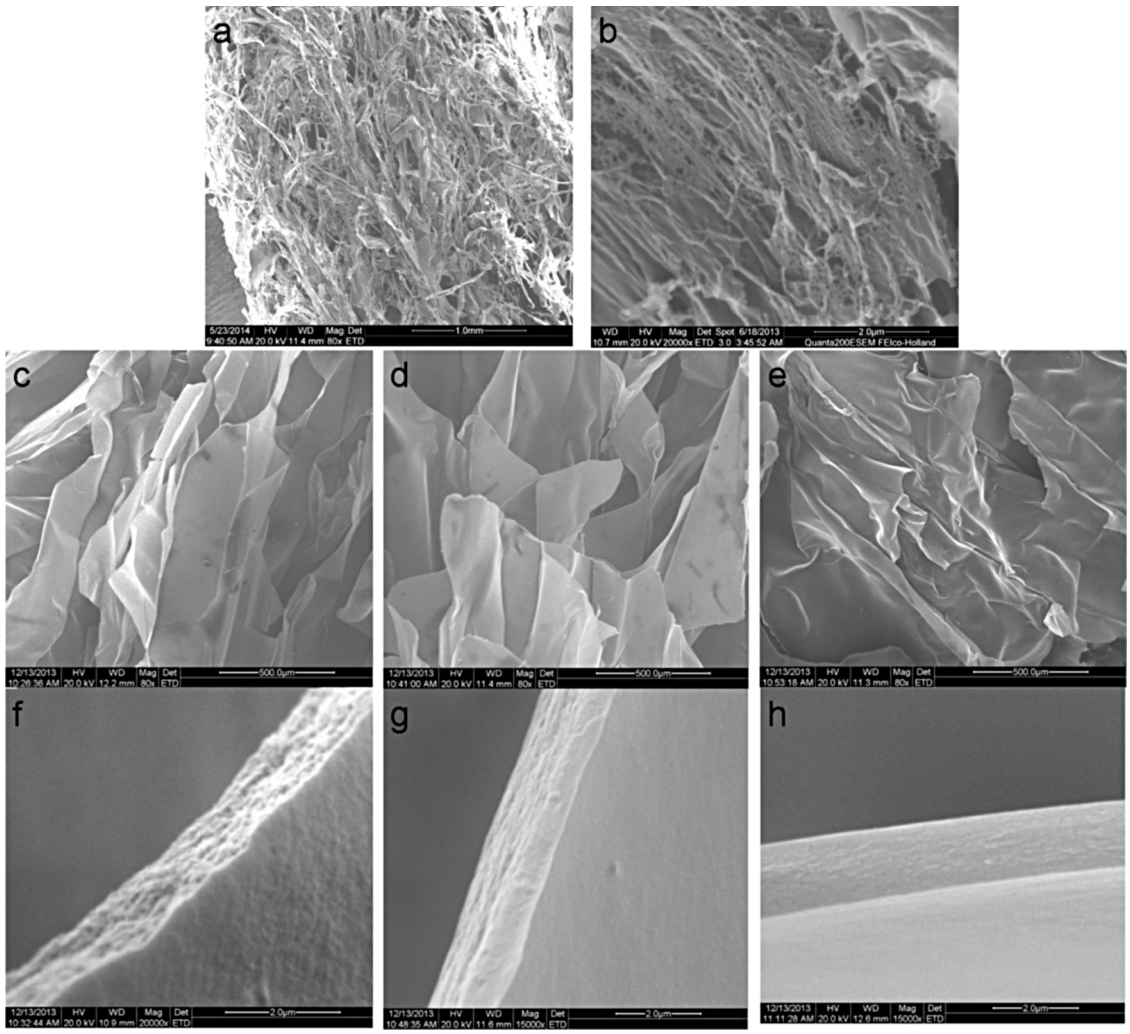

Fig. 2. (a)–(e) Are the SEM images of cellulose self-assemblies with different MBA amount, i.e., $r = 0$, 0.2, 0.375, 0.473, 0.545, respectively. (f)-(h) are the magnified images of (c)–(e), respectively.

increase due to the cross-linkage of MBA on cellulose. However, as MBA is excess (r above 0.473), it becomes unfavorable to the absorption of water instead because too much hydroxyl groups are consumed. From Fig. S3, there is a maximum water uptake ratio as much as 99.6% (260 g/g $w_{water}/w_{cellulose}$) when r reaches 0.473. The actual photographs in Fig. S3 intuitively display the volume change of cellulose hydrogels, also reflecting the hydrogel has maximum water uptake capability at $r = 0.473$.

3.2. Fabrication of 3D ordered films, and the structure and strength properties

As mentioned above, cellulose sheets tend to be formed with the assistance of cross-linkage of MBA during evaporation. The structural feature inspires us to fabricate a highly ordered 3D structure by diecasting these 2D cellulose sheets. The primary strategy to fabricate an ordered cellulose 3D structure is as shown in Fig. 4. It can be imagined that most of sheets formed in cellulose aerogels would not be parallel spontaneously with each other without external pressure. During the evaporating process, a normal pressure exerting upon the cellulose hydrogel with two parallel plates would induce nearly all cellulose sheets to align in parallel with the parallel plates. Moreover, folding deformation of cellulose sheets has to occur under the external pressure to keep sheet segments parallel with each other. Therefore, no matter in whatever orientation cellulose sheets used to be, all cellulose sheet segments would be rearranged in parallel under external normal pressure, resulting in a highly ordered structure, so called 'brickwork'. Fig. 4 shows a rectangular cellulose hydrogel, as well as a dry cellulose film from evaporating the hydrogel under a normal pressure, and also shows a typical SEM image of a cross-section of a dry cellulose film. It can be seen that the cellulose film is constructed by stacking of many close-packed layers. Moreover, in the figure, lots of defects of stripe patterns distribute within the cellulose film, also reflecting the lamellar stacking in the 3D cellulose film. It should be noted here that the ordered films with close-stacked cellulose layers are not acquired via freeze–drying, indicating freeze–drying is not necessary to fabricate cellulose sheets as reported elsewhere (Han et al., 2013).

As is well-known, the strength properties of materials are tightly related to their structures. As a result of rearrangement of cellulose sheets into 3D ordered cellulose films under an external pressure, the strength properties of cellulose films are greatly improved. Fig. 5 shows the stress of three typical cellulose films as a function of strain. It is proved that only when r reaches 0.375, where cellulose sheets would be acquired and 3D ordered cellulose films would be formed, can the strength properties of cellulose films be improved greatly. From the curves, the tensile strength (σ) has been enhanced significantly from ~60 MPa to ~135 MPa as r increases from 0.375 to 0.473. Obviously,

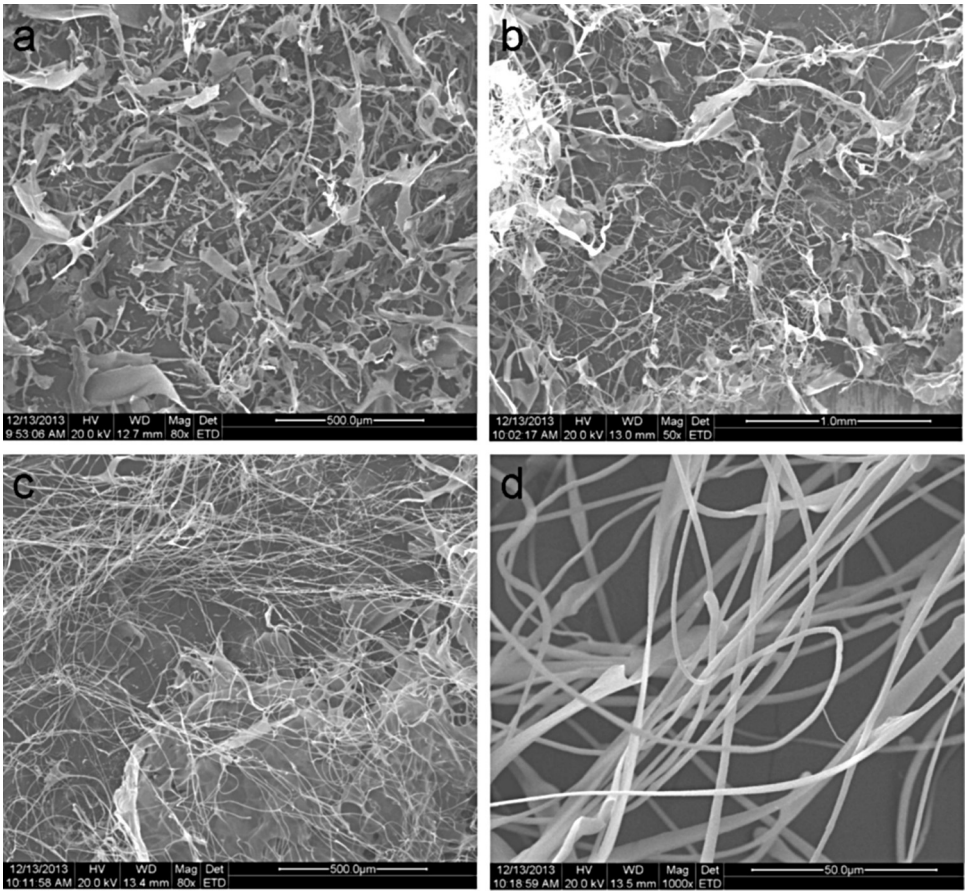

Fig. 3. SEM images of cellulose self-assemblies for diluted cellulose dispersions, indicating the morphological transition with increasing CLD. (a)–(c) Correspond to samples H1–H3, respectively, and (d) is a SEM image of H3 at higher magnification.

compared with other regenerated cellulose materials (Geng et al., 2014), the ordered 3D cellulose films exhibit giant improvement in tensile strength. Accordingly, the value of strain to failure (ε) is also enhanced significantly, from 10% to 25%, reflecting an excellent flexibility. It is inferred that high tensile strength of cellulose films could be attributed to the ordered arrangement of cellulose sheets. At the same time, the relative sliding between these parallel cellulose sheets could occur, bringing the high malleability and excellent toughness to the ordered cellulose films.

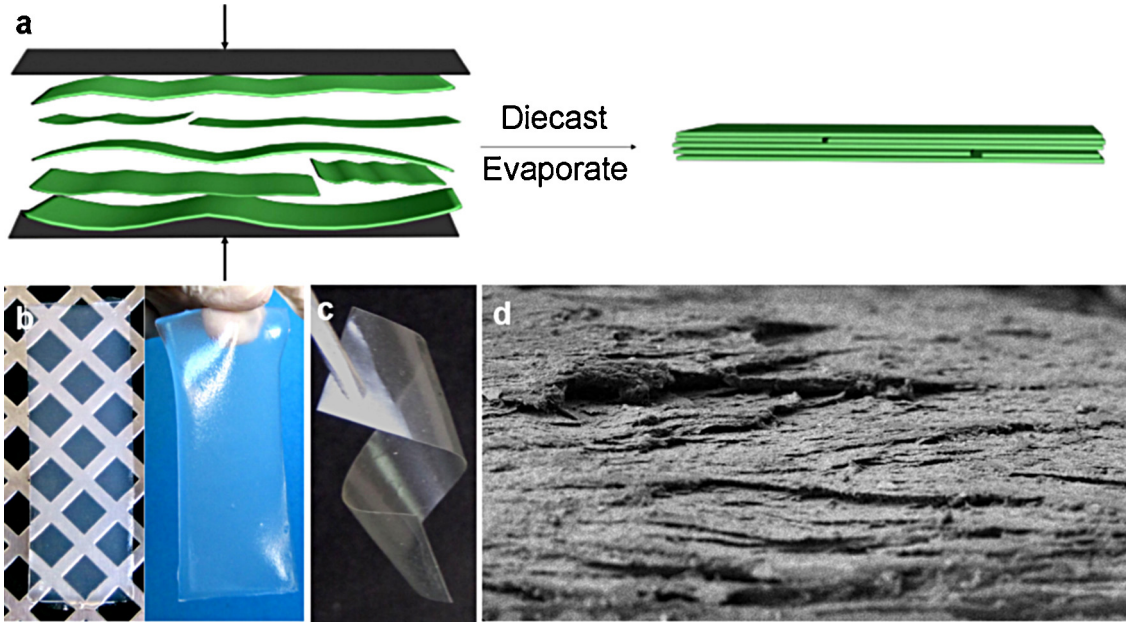

Fig. 4. (a) Schematic diagram of preparation of ordered 3D cellulose films under a normal pressure through evaporation; (b) photographs of a retangular cellulose hydrogel formed by using templating method; a dry cellulose film (c) prepared through evaporation; (d) a SEM image of the cross-section of a dry cellulose film.

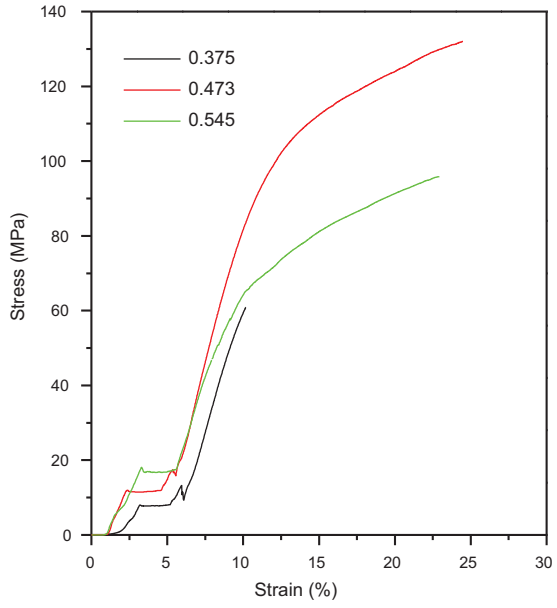

Fig. 5. The stress of cellulose films at $r = 0.375$, 0.473, and 0.545 as a function of strain.

Here, we propose that it is the ordered structure but not the chemical cross-linkage between cellulose and MBA that should be responsible for high-strength properties of the cellulose films. As for this point, it can be analyzed from the film samples with larger r. Fig. 5 shows that when the amount of MBA increases to the point $r = 0.545$, the strength property greatly reduces from 130 MPa to 90 MPa. Therefore, it can be deduced that in the cellulose film materials, although the cross-linkage of MBA helps build the ordered structures, it does not decide the excellent strength properties.

4. Conclusions

Cellulose hydrogels are prepared through cross-linkage of dissolved cellulose in a green aqueous solvent media. The cellulose hydrogels exhibit high water uptake capability with maximum water uptake ratio up to 99.6%. The dispersions of cellulose hydrogels could self-assemble into perfect sheets and high-aspect-ratio fibers by controlling the content of MBA and cellulose concentration. Through diecasting and evaporating cellulose hydrogels, 3D ordered cellulose films with closely stacking of cellulose sheets are fabricated. The ordered structure of cellulose endows the films excellent tensile strength and flexibility. This work is expected to open up a simple approach of manufacturing high-strength ordered cellulose materials.

Acknowledgements

The authors would like to thank the China Postdoctoral Science Foundation (2012M511491) and Shandong Province Young and Middle-Aged Scientists Research Awards Fund (BS2012CL030), the National Natural Science Foundation of China (31370581) and the Program for the Scholar of Yellow River Mouth (DYRC20120105) for financial support.

Appendix A. Supplementary data

Supplementary data associated with this article can be found, in the online version, at http://dx.doi.org/10.1016/j.carbpol.2014.10.003.

References

Cai, J., Liu, S., Feng, J., Kimura, S., Wada, M., Kuga, S., et al. (2012). Cellulose-silica nanocomposite aerogels by in situ formation of silica in cellulose gel. *Angewandte Chemie International Edition*, *124*(9), 2118–2121.
Cai, J., & Zhang, L. (2005). Rapid dissolution of cellulose in LiOH/urea and NaOH/urea aqueous solutions. *Macromolecular Bioscience*, *5*(6), 539–548.
Cai, J., & Zhang, L. (2006). Unique gelation behavior of cellulose in NaOH/urea aqueous solution. *Biomacromolecules*, *7*(1), 183–189.
Cai, J., Zhang, L., Liu, S., Liu, Y., Xu, X., Chen, X., et al. (2008). Dynamic self-assembly induced rapid dissolution of cellulose at low temperatures. *Macromolecules*, *41*(23), 9345–9351.
Chang, C., Duan, B., & Zhang, L. (2009). Fabrication and characterization of novel macroporous cellulose–alginate hydrogels. *Polymer*, *50*(23), 5467–5473.
Chen, W., Yu, H., Li, Q., Liu, Y., & Li, J. (2011). Ultralight and highly flexible aerogels with long cellulose I nanofibers. *Soft Matter*, *7*(21), 10360–10368.
Eichhorn, S. J. (2012). Stiff as a board: Perspectives on the crystalline modulus of cellulose. *ACS Macro Letters*, *1*(11), 1237–1239.
Fox, J., Wie, J. J., Greenland, B. W., Burattini, S., Hayes, W., Colquhoun, H. M., et al. (2012). High-strength, healable, supramolecular polymer nanocomposites. *Journal of the American Chemical Society*, *134*(11), 5362–5368.
Geng, H., Yuan, Z., Fan, Q., Dai, X., Zhao, Y., Wang, Z., et al. (2014). Characterisation of cellulose films regenerated from acetone/water coagulants. *Carbohydrate Polymers*, *102*, 438–444.
Giese, M., De Witt, J. C., Shopsowitz, K. E., Manning, A. P., Dong, R. Y., Michal, C. A., et al. (2013). Thermal switching of the reflection in chiral nematic mesoporous organosilica films infiltrated with liquid crystals. *ACS Applied Materials & Interfaces*, *5*(15), 6854–6859.
Habibi, Y., Chanzy, H., & Vignon, M. R. (2006). TEMPO-mediated surface oxidation of cellulose whiskers. *Cellulose*, *13*(6), 679–687.
Han, J., Zhou, C., Wu, Y., Liu, F., & Wu, Q. (2013). Self-assembling behavior of cellulose nanoparticles during freeze–drying: Effect of suspension concentration, particle size, crystal structure, and surface charge. *Biomacromolecules*, *14*(5), 1529–1540.
He, M., Xu, M., & Zhang, L. (2013). Controllable stearic acid crystal induced high hydrophobicity on cellulose film surface. *ACS Applied Materials & Interfaces*, *5*(3), 585–591.
He, M., Zhao, Y., Duan, J., Wang, Z., Chen, Y., & Zhang, L. (2014). Fast contact of solid–liquid interface created high strength multi-layered cellulose hydrogels with controllable size. *ACS Applied Materials & Interfaces*, *6*(3), 1872–1878.
Heath, L., & Thielemans, W. (2010). Cellulose nanowhisker aerogels. *Green Chemistry*, *12*(8), 1448–1453.
Kroon-Batenburg, L., & Kroon, J. (1997). The crystal and molecular structures of cellulose I and II. *Glycoconjugate Journal*, *14*(5), 677–690.
Kulpinski, P. (2005). Cellulose nanofibers prepared by the *N*-methylmorpholine-*N*-oxide method. *Journal of Applied Polymer Science*, *98*(4), 1855–1859.
Langan, P., Nishiyama, Y., & Chanzy, H. (1999). A revised structure and hydrogen-bonding system in cellulose II from a neutron fiber diffraction analysis. *Journal of the American Chemical Society*, *121*(43), 9940–9946.
Li, R., Chang, C., Zhou, J., Zhang, L., Gu, W., Li, C., et al. (2010). Primarily industrialized trial of novel fibers spun from cellulose dope in NaOH/urea aqueous solution. *Industrial and Engineering Chemistry Research*, *49*(22), 11380–11384.
Liu, S., Zhang, L., Zhou, J., Xiang, J., Sun, J., & Guan, J. (2008). Fiberlike Fe_2O_3 macroporous nanomaterials fabricated by calcinating regenerate cellulose composite fibers. *Chemistry of Materials*, *20*(11), 3623–3628.
Moon, R. J., Martini, A., Nairn, J., Simonsen, J., & Youngblood, J. (2011). Cellulose nanomaterials review: Structure, properties and nanocomposites. *Chemical Society Reviews*, *40*(7), 3941–3994.
Morandi, G., Heath, L., & Thielemans, W. (2009). Cellulose nanocrystals grafted with polystyrene chains through surface-initiated atom transfer radical polymerization (SI-ATRP). *Langmuir*, *25*(14), 8280–8286.
Nishiyama, Y., Langan, P., & Chanzy, H. (2002). Crystal structure and hydrogen-bonding system in cellulose Iβ from synchrotron X-ray and neutron fiber diffraction. *Journal of the American Chemical Society*, *124*(31), 9074–9082.
Roder, T., Morgenstern, B., Schelosky, N., & Glatter, O. (2001). Solutions of cellulose in *N*,*N*-dimethylacetamide/lithium chloride studied by light scattering methods. *Polymer*, *42*(16), 6765–6773.
Saito, T., Uematsu, T., Kimura, S., Enomae, T., & Isogai, A. (2011). Self-aligned integration of native cellulose nanofibrils towards producing diverse bulk materials. *Soft Matter*, *7*(19), 8804–8809.
Shahin, A., Nicolai, T., Benyahia, L., Tassin, J.-F., & Chassenieux, C. (2013). Evidence for the coexistence of interpenetrating permanent and transient networks of hydroxypropyl methyl cellulose. *Biomacromolecules*, *15*(1), 311–318.
Shi, X., Zhang, L., Cai, J., Cheng, G., Zhang, H., Li, J., et al. (2011). A facile construction of supramolecular complex from polyaniline and cellulose in aqueous system. *Macromolecules*, *44*(12), 4565–4568.
Shopsowitz, K. E., Hamad, W. Y., & MacLachlan, M. J. (2012). Flexible and iridescent chiral nematic mesoporous organosilica films. *Journal of the American Chemical Society*, *134*(2), 867–870.
Shopsowitz, K. E., Qi, H., Hamad, W. Y., & MacLachlan, M. J. (2010). Free-standing mesoporous silica films with tunable chiral nematic structures. *Nature*, *468*(7322), 422–425.

Šturcová, A., Davies, G. R., & Eichhorn, S. J. (2005). Elastic modulus and stress-transfer properties of tunicate cellulose whiskers. *Biomacromolecules*, *6*(2), 1055–1061.
Sun, W., Sun, D., Wei, Y., Liu, S., & Zhang, S. (2007). Oil-in-water emulsions stabilized by hydrophobically modified hydroxyethyl cellulose: Adsorption and thickening effect. *Journal of Colloid and Interface Science*, *311*(1), 228–236.
Swatloski, R. P., Spear, S. K., Holbrey, J. D., & Rogers, R. D. (2002). Dissolution of cellose with ionic liquids. *Journal of the American Chemical Society*, *124*(18), 4974–4975.
Zhang, L., Mao, Y., Zhou, J., & Cai, J. (2005). Effects of coagulation conditions on the properties of regenerated cellulose films prepared in NaOH/urea aqueous solution. *Industrial and Engineering Chemistry Research*, *44*(3), 522–529.
Zhu, S., Wu, Y., Chen, Q., Yu, Z., Wang, C., Jin, S., et al. (2006). Dissolution of cellulose with ionic liquids and its application: A mini-review. *Green Chemistry*, *8*(4), 325–327.